

Ultrafast Growth of Highly Ordered Anodic TiO₂ Nanotubes in Lactic Acid Electrolytes

Seulgi So, Kiyong Lee, and Patrik Schmuki*

Department of Materials Science, WW4-LKO, University of Erlangen-Nuremberg, Martensstrasse 7, 91058 Erlangen, Germany

S Supporting Information

ABSTRACT: In the present work, we show that fully functional self-organized TiO₂ nanotube layers can be electrochemically grown with an unprecedented growth rate if lactic acid (LA) is used as an additive during anodization. The main effect of LA addition is that it allows performing nanotube growth at significantly higher anodization voltage than in the LA free case, and this without dielectric oxide breakdown (“burning”). As a result, for example, 15 μm tube thick nanotube layers, suitable for a use in dye-sensitized solar cells (DSSCs) can be grown in 45 s and 7 μm tubes suitable for water splitting can be grown in 25 s.

Over the past decade, aligned TiO₂ nanotube arrays that are grown on a metallic Ti substrate by self-organizing anodization have attracted tremendous scientific interest (for an overview see, e.g., ref 1a). This is mainly due to the high expectations in view of their application in classic TiO₂-fields, such as biomedical devices,¹ photocatalysts,² photoelectrochemical water splitting (PWS),³ or dye-sensitized solar cells (DSSCs).⁴ The performance of the tube layers in DSSCs and in PWS depends on a number of parameters, such as ordering, diameter, and length of the tubes.^{4e,h} Optimum performance is usually found for hexagonally ordered tubes with a length of 15–20 μm in DSSCs,^{4e,j,5} or ≈7 μm in PWS^{3b} when investigated under artificial solar irradiation (AM 1.5) conditions (see also Supporting Information (SI), Figure S1).

Since the first reports on anodic TiO₂ nanotube synthesis in dilute fluoride electrolytes by Zwillig et al. in 1999,⁶ who grew comparably irregular tube morphologies with a limited thickness of ≈500 nm, rapid improvement in growth techniques has been established toward longer, and much more ordered nanotube layers,⁷ such as shown in Figure 1a. In particular, the introduction of organic electrolytes and the fine-tuning of fluoride and water content in the electrolyte were crucial, not only in view of tube geometry, but also regarding the properties of the layers.⁷

Today, most common for TiO₂ nanotube growth are NH₄F–water–EG electrolytes that are routinely used for fabricating tube arrays for solar cell or water splitting applications. The anodization time to grow tubes of a suitable length and quality for DSSCs and PWS is mainly determined by the applied voltage and the electrolyte composition. For example, in order to form a 15 μm thick layer suitable for DSSCs,^{4j,e,5} using classic recipes it took over 2 h; while most recent recipes led to

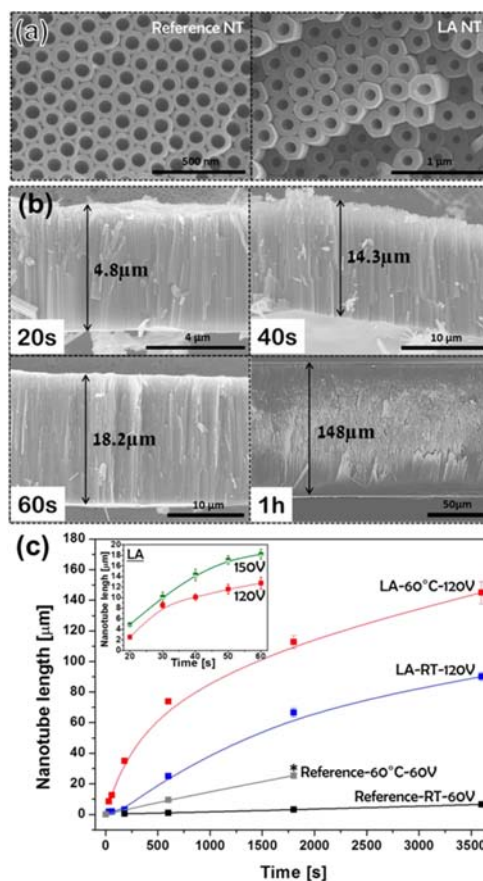


Figure 1. (a) Morphology of TiO₂ nanotube layers formed under “classic” condition in a 0.1 M NH₄F–5 wt % H₂O–EG electrolyte (left) and in the same electrolyte with lactic acid (LA) addition (right). The SEM images show a top view on the ordered morphologies. (b) Cross-sectional SEM images of a tube layer grown in the LA electrolyte at 150 V (first three) and 120 V (last) showing the rapid growth in the LA electrolyte. (c) Comparison of nanotube length vs time in LA containing electrolytes compared with the LA-free case. *Reference tubes under these conditions show deterioration of their morphology, see SI Figure S2.

fastest reported growth rates that could grow 16 μm tubes in 10 min.⁸

In the present paper, we report an anodization approach that yields an unprecedented growth rate for ordered TiO₂

Received: February 26, 2012

Published: June 22, 2012

nanotubes; it is based on the “field supporting effect” of a weak organic acid, LA. As a result, 15 μm long highly ordered tube layers for solar cells can be grown in ≈ 45 s, and 7 μm long tubes for water splitting in ≈ 25 s (see Figure 1).

Mechanistically, the growth rate determining factor for a classic high field anodization process (largely explored to form compact anodic films)⁹ is that a high driving voltage can be established across the growing oxide without causing local dielectric breakdown events (e.g., avalanche breakdown or “burning”).^{9,10} The threshold voltage for “burning” depends among other factors on the ionic species present in the electrolyte. Some specific additives to the electrolyte (namely, weak organic acids such as oxalic acid, citric acid, malonic acid, glycolic acid, etc.) are known empirically¹¹ to shift the threshold voltage to a significantly higher value and thus allow to achieve a higher thickness of a compact film or a more rapid anodization process (additional discussion is given in SI, S3). This prompted us to screen a range of most promising candidates to be used as additives to the TiO_2 tube-growth electrolytes. A compilation of a number of experimental conditions and additives explored is given in the SI (Figure S2). While some additives such as glycolic acid, citric acid, and EDTA showed beneficial effects, we found a most outstanding anodization behavior by the addition of LA.

Figure 1 illustrates the effect on growth rate using an addition of 1.5 M LA to a standard anodization electrolyte (0.1 M NH_4F –5 wt % H_2O –EG). In the LA–electrolyte, anodization can be carried out at voltages as high as at 120–150 V, while electrolytes without this addition show, at these voltages, oxide breakdown (Figure 2) or severe tube damage (some examples are shown in SI Figure S2). The SEM images shown in Figure 1b give the sequence of the tube length evolution with time using the LA–electrolyte (more detailed SEM sequences are shown in SI Figure S4). Figure 1c compares the growth rates of TiO_2 nanotubes in the LA electrolyte to the LA free case. It is apparent that in the reference electrolyte (0.1 M NH_4F –5 wt % H_2O –EG), for example, a length of 15 μm is achieved after 2.5 h, while for LA addition, the growth time is 45 s (see inset of Figure 1c), that is, the rate is accelerated by a factor of 200.

In spite of the accelerated growth, the morphology of the nanotubes and the degree of order resemble the best cases for classic electrolytes (Figure 1a, right).

Figure 2 illustrates that the effect of LA is mainly the prevention of anodic breakdown at high anodization voltages. Figure 2a shows the current versus time characteristics at an anodization voltage of 120 V with and without LA in the electrolyte. In the LA case, the desired growth–dissolution equilibrium can be established after an initiation phase; that is, after an initial rise, the current drops to a steady state value with continuous tube growth (this current–time behavior is typical for optimized self-organizing systems). In the LA free case, the current rises fast and continuously, while at the same time, local breakdown at distinct sites on the samples can be observed (Figure 2b). The findings are in line with considerable amount of general anodization literature.¹²

Higher breakdown voltages are often observed for species showing suitable anchoring groups to form (mono) layers on the corresponding oxides.^{11b,c,12a,13} This is also observed for LA: the ToF-SIMS spectra in Figure 2c show the molecular fragment M–H as well as the condensation product with Ti–OH for anodization in LA. The latter indicates adsorption and strong bond formation in line with XPS data in the SI (Figure S3a). This supports the concept that strongly adsorbing species

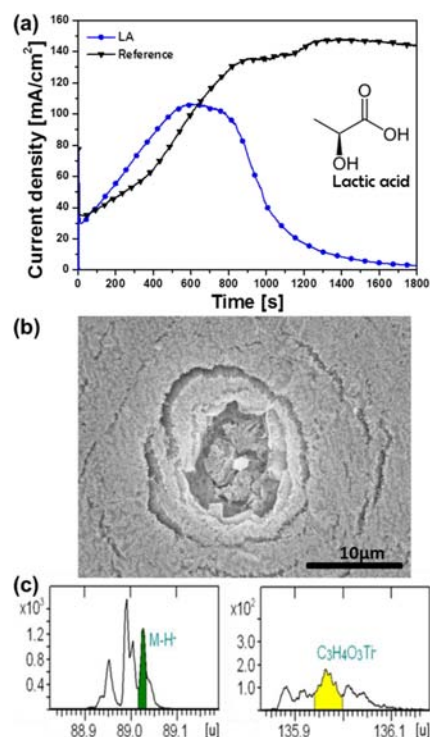


Figure 2. (a) Current–time behavior for anodization at 120 V in LA electrolyte and reference electrolyte at RT. (b) Typical breakdown morphology in reference electrolyte observed after short time at 120 V when tube layer is first formed at 60 V and voltage then is increased to 120 V. (c) Identification of LA adsorption on TiO_2 by ToF-SIMS analysis of compact oxide layer formed in LA-containing electrolyte showing M–H fragment (left) and TiO^- condensation product (right).

can prevent breakdown during anodization reactions (see also additional discussion in the SI, S3). In view of composition and structure, the tubes formed under ultrafast conditions show the same characteristics as reference tubes; that is, in XRD and XPS, tubes formed in LA show identical characteristics as the reference tubes (SI, Figure S5).

To demonstrate the same level of functionality for the LA grown tubes and conventionally grown tubes, we compared both tube types in two of their main applications, DSSCs and PWS (Figure 3). For DSSCs, we neither used front side illumination concepts¹⁴ nor additional area increasing measures such as TiCl_4 treatments.¹⁵ Therefore, the absolute efficiencies of the solar cells are comparably low,^{14,15} but the intention is to compare the plain tube properties without convolution of the data. From the results, it is clear that the ultrarapidly grown tube layers show an at least as high efficiency as the classic reference tubes in both applications.

In summary, the main achievement of the present work is to provide an exceptionally effective additive to the currently most used anodization electrolyte to grow self-organizing TiO_2 nanotube layers. We show that LA can effectively prevent localized dielectric breakdown of the anodic oxide at elevated anodization voltages; thus, it allows establishing a higher ion transport through the oxide film and, as a result, achieves extremely fast tube growth rates without losing the tube’s functional properties. It is noteworthy that the beneficial effect is in line with chelating properties of LA^{11a,16} and surface complex formation that may drastically affect the breakdown voltage during anodization (please see the SI for more discussion).

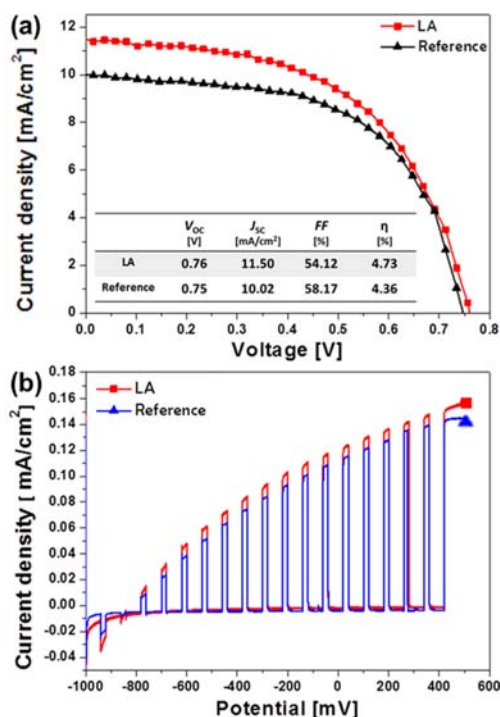


Figure 3. (a) I–V characteristics for DSSCs fabricated using reference nanotube and LA nanotube samples (both of a tube length of 15 μm) annealed at 450 $^{\circ}\text{C}$, 3 h. (J_{SC} = short-circuit current, V_{OC} = open-circuit voltage, FF = fill factor, η = efficiency). (b) Water splitting experiment light/dark I–V curve taken in 1 M KOH using reference nanotube and LA nanotube samples (both of a length of 7 μm) annealed at 650 $^{\circ}\text{C}$, 3 h. Both experiments were carried out using AM 1.5 (100 mW/cm^2) illumination conditions.

■ ASSOCIATED CONTENT

● Supporting Information

Experimental details, anodic breakdown mechanism, current density transients, screen a range of candidates as additives, SEM images, XRD, and XPS of the samples. This material is available free of charge via the Internet at <http://pubs.acs.org>.

■ AUTHOR INFORMATION

Corresponding Author

schmuki@ww.uni-erlangen.de

Notes

The authors declare no competing financial interest.

■ ACKNOWLEDGMENTS

The authors would like to acknowledge DFG and the Erlangen DFG cluster of excellence for financial support. We thank Manuela Killian for ToF-SIMS measurements.

■ REFERENCES

- (1) (a) Roy, P.; Berger, S.; Schmuki, P. *Angew. Chem., Int. Ed.* **2011**, *50*, 2904. (b) Park, J.; Bauer, S.; Von Der Mark, K.; Schmuki, P. *Nano Lett.* **2007**, *7*, 1686. (c) Oh, S. H.; Finônes, R. R.; Daraio, C.; Chen, L. H.; Jin, S. *Biomaterials* **2005**, *26*, 4938.
- (2) (a) Macak, J. M.; Zlamal, M.; Krysa, J.; Schmuki, P. *Small* **2007**, *3*, 300. (b) Fujishima, A.; Rao, T. N.; Tryk, D. A. *J. Photochem. Photobiol., C* **2000**, *1*, 1. (c) Kato, H.; Kudo, A. *J. Phys. Chem. B* **2002**, *106*, 5029. (d) Liu, Z.; Zhang, X.; Nishimoto, S.; Murakami, T.; Fujishima, A. *Environ. Sci. Technol.* **2008**, *42*, 8547.
- (3) (a) Park, J. H.; Kim, S.; Bard, A. J. *Nano Lett.* **2006**, *6*, 24. (b) Das, C.; Roy, P.; Yang, M.; Jha, H.; Schmuki, P. *Nanoscale* **2011**, *3*,

3094. (c) Fujishima, A.; Honda, K. *Nature* **1972**, *238*, 37. (d) Mor, G. K.; Shankar, K.; Paulose, M.; Varghese, O. K.; Grimes, C. A. *Nano Lett.* **2005**, *5*, 191. (e) Fujishima, A.; Zhang, X.; Tryk, D. A. *Surf. Sci. Rep.* **2008**, *63*, 515. (f) Maeda, K.; Domen, K. *J. Phys. Chem. Lett.* **2010**, *1*, 2655. (g) Roy, P.; Das, C.; Lee, K.; Hahn, R.; Ruff, T.; Moll, M.; Schmuki, P. *J. Am. Chem. Soc.* **2011**, *133*, 5629. (h) Lynch, R. P.; Ghicov, A.; Schmuki, P. *J. Electrochem. Soc.* **2010**, *157*, G76.

- (4) (a) Grätzel, M. *Nature* **2001**, *414*, 338. (b) Macák, J. M.; Tsuchiya, H.; Ghicov, A.; Schmuki, P. *Electrochem. Commun.* **2005**, *7*, 1133. (c) Mor, G. K.; Shankar, K.; Paulose, M.; Varghese, O. K.; Grimes, C. A. *Nano Lett.* **2006**, *6*, 215. (d) Kopidakis, N.; Benkstein, K. D.; Van De Lagemaat, J.; Frank, A. J. *J. Phys. Chem. B* **2003**, *107*, 11307. (e) Roy, P.; Kim, D.; Lee, K.; Spiecker, E.; Schmuki, P. *Nanoscale* **2010**, *2*, 45. (f) Jennings, J. R.; Ghicov, A.; Peter, L. M.; Schmuki, P.; Walker, A. B. *J. Am. Chem. Soc.* **2008**, *130*, 13364. (g) Zhu, K.; Neale, N. R.; Miedaner, A.; Frank, A. J. *Nano Lett.* **2007**, *7*, 69. (h) Zhu, K.; Vinzant, T. B.; Neale, N. R.; Frank, A. J. *Nano Lett.* **2007**, *7*, 3739. (i) Kim, J. Y.; Noh, J. H.; Zhu, K.; Halverson, A. F.; Neale, N. R.; Park, S.; Hong, K. S.; Frank, A. J. *ACS Nano* **2011**, *5*, 2647. (j) Ghicov, A.; Albu, S. P.; Hahn, R.; Kim, D.; Stergiopoulos, T.; Kunze, J.; Schiller, C. A.; Falaras, P.; Schmuki, P. *Chem.—Asian. J.* **2009**, *4*, 520.

- (5) Hsiao, P. T.; Liou, Y. J.; Teng, H. *J. Phys. Chem. C* **2011**, *115*, 15018.

- (6) Zwilling, V.; Darque-Ceretti, E.; Boutry-Forveille, A.; David, D.; Perrin, M. Y.; Aucouturier, M. *Surf. Interface Anal.* **1999**, *27*, 629.

- (7) (a) Macak, J. M.; Tsuchiya, H.; Taveira, L.; Aldaberggerova, S.; Schmuki, P. *Angew. Chem., Int. Ed.* **2005**, *44*, 7463. (b) Vasilev, K.; Poh, Z.; Kant, K.; Chan, J.; Michelmore, A.; Losic, D. *Biomaterials* **2010**, *31*, 532. (c) Albu, S. P.; Roy, P.; Virtanen, S.; Schmuki, P. *Isr. J. Chem.* **2010**, *50*, 453.

- (8) (a) Yin, H.; Liu, H.; Shen, W. Z. *Nanotechnology* **2010**, *21*, 035601. (b) Sreekantan, S.; Wei, L. C.; Lockman, Z. *J. Electrochem. Soc.* **2011**, *158*, C397. (c) Liao, Y.; Que, W. *J. Alloys Compd.* **2010**, *505*, 243. (d) Sreekantan, S.; Saharudin, K. A.; Lockman, Z.; Tzu, T. W. *Nanotechnology* **2010**, *21*, 265603. (e) Hu, A.; Li, H.; Jia, Z.; Xia, Z. *J. Solid State Chem.* **2011**, *184*, 2936.

- (9) Vanhumbecq, J. F.; Proost, J. *Corros. Rev.* **2009**, *27*, 117.

- (10) (a) Ono, S.; Saito, M.; Asoh, H. *Electrochem. Solid-State Lett.* **2004**, *7*, B21. (b) Yasuda, K.; Macak, J. M.; Berger, S.; Ghicov, A.; Schmuki, P. *J. Electrochem. Soc.* **2007**, *154*, C472.

- (11) (a) St, C. J. D.; Delpesco, T. W. U.S. 6 737 485 B1, 2004. (b) Liu, Y.; Scheuer, C. US20050218005A1, 2005. (c) Fernandez, M.; Baonza, J.; Albella, J. M.; Martinez-Duart, J. M. *Electrocomp. Sci. Technol.* **1981**, *7*, 205.

- (12) (a) Aerts, T.; De Graeve, I.; Terryn, H. *Electrochim. Acta* **2008**, *54*, 270. (b) Young, L. *Anodic Oxide Films*; Academic Press: New York, 1961. (c) Albella, J. M.; Montero, I.; Martínez-Duart, J. M.; Parkhutik, V. *J. Mater. Sci.* **1991**, *26*, 3422.

- (13) (a) Di Quarto, F.; Piazza, S.; Sunseri, C. *J. Electroanal. Chem.* **1988**, *248*, 99. (b) Liu, Y.; Goad, D.; Budek, D.; Scheuer, C. EP1826297A2, 2007.

- (14) Park, J. H.; Lee, T. W.; Kang, M. G. *Chem. Commun.* **2008**, 2867.

- (15) (a) Roy, P.; Kim, D.; Paramasivam, I.; Schmuki, P. *Electrochem. Commun.* **2009**, *11*, 1001. (b) Nazeeruddin, M. K.; Humphry-Baker, R.; Liska, P.; Grätzel, M. *J. Phys. Chem. B* **2003**, *107*, 8981.

- (16) Kakihana, M.; Tomita, K.; Petrykin, V.; Tada, M.; Sasaki, S.; Nakamura, Y. *Inorg. Chem.* **2004**, *43*, 4546.